PLOS ONE

RESEARCH ARTICLE

Rotating Flow of Magnetite-Water Nanofluid over a Stretching Surface Inspired by Non-Linear Thermal Radiation

M. Mustafa[1]*, A. Mushtaq[2], T. Hayat[3,4], A. Alsaedi[4]

1 School of Natural Sciences (SNS), National University of Sciences and Technology (NUST), Islamabad, 44000, Pakistan, **2** Research Centre for Modeling and Simulation (RCMS), National University of Sciences and Technology (NUST), Islamabad, 44000, Pakistan, **3** Department of Mathematics, Quaid-I-Azam University 45320, Islamabad, 44000, Pakistan, **4** Nonlinear Analysis and Applied Mathematics (NAAM) Research Group, Department of Mathematics, Faculty of Science, King Abdulaziz University, Jeddah, 21589, Saudi Arabia

* meraj_mm@hotmail.com

Citation: Mustafa M, Mushtaq A, Hayat T, Alsaedi A (2016) Rotating Flow of Magnetite-Water Nanofluid over a Stretching Surface Inspired by Non-Linear Thermal Radiation. PLoS ONE 11(2): e0149304. doi:10.1371/journal.pone.0149304

Editor: Xiao-Dong Wang, North China Electric Power University, CHINA

Received: October 4, 2015

Accepted: January 29, 2016

Published: February 19, 2016

Data Availability Statement: All relevant data are within the paper.

Funding: The authors have no support or funding to report.

Competing Interests: The authors have declared that no competing interests exist.

Abstract

Present study explores the MHD three-dimensional rotating flow and heat transfer of ferrofluid induced by a radiative surface. The base fluid is considered as water with magnetite-Fe_3O_4 nanoparticles. Novel concept of non-linear radiative heat flux is considered which produces a non-linear energy equation in temperature field. Conventional transformations are employed to obtain the self-similar form of the governing differential system. The arising system involves an interesting temperature ratio parameter which is an indicator of small/large temperature differences in the flow. Numerical simulations with high precision are determined by well-known shooting approach. Both uniform stretching and rotation have significant impact on the solutions. The variation in velocity components with the nanoparticle volume fraction is non-monotonic. Local Nusselt number in Fe_3O_4–water ferrofluid is larger in comparison to the pure fluid even at low particle concentration.

Introduction

The study of flow in a rotating frame is motivated in view of its theoretical and practical significance in geophysics and engineering. Prominent geophysical applications include the magma flow in earth's mantle close to earth crust and flows in geological formations subject to earth rotation. The engineering applications of such flows exist in chemical and food processing industry, centrifugal filtration process, rotating machinery and design of multi-pore distributor in a gas-solid fluidized bed. Pioneering study on the three-dimensional rotating viscous flow induced by a stretching surface was presented by Wang [1]. His problem was governed by an interesting parameter λ that signifies the ratio of the rotation to the stretching rate. He constructed series solutions for small values of parameter λ by regular perturbation approach. He found that velocity distribution (above the sheet) decreases upon increasing this parameter λ. Rajeswari and Nath [2] and Nazar et al. [3] extended the Wang's work for unsteady case. Their

results indicate a smooth transition from initial unsteady flow to final steady-state flow. Homotopy solutions for rotating flow of non-Newtonian second grade fluid were provided by Hayat et al. [4]. They observed that fluid velocity has direct relationship with material parameter of second grade fluid. Zaimi et al. [5] examined the rotating flow of viscoelastic fluid bounded by a stretching surface and concluded that boundary layer thickness is an increasing function of viscoelastic fluid parameter. Rashidi et al. [6] investigated entropy generation in steady MHD flow due to a rotating porous disk in a nanofluid. Sheikholeslami et al. [7] reported numerical results of nanofluid flow and heat transfer in a rotating system with the consideration of magnetic field effects. Mustafa [8] used Cattaneo-Christov heat flux model to investigate the rotating flow of viscoelastic fluid bounded by a stretching surface.

Cooling capabilities of heat transfer equipment have been constrained because of the low thermal conductivity of conventional coolants including water, oil and ethylene glycol. It is well known that thermal conductivity of metals is very high as compared to that of liquids. Thus one of effective approaches to enhance heat transfer performance is via dispersing tiny metallic particle of nanometer dimensions in the liquids. Choi [9] was the first to introduce the terminology of nanofluids. Sheikholeslami and Ganji [10] considered the MHD flow and heat transfer inside a semi annulus enclosure having sinusoidal hot wall. They used Maxwell models to estimate the effective thermal conductivity and effective electrical conductivity of the nanofluids. Turkyilmazoglu [11] examined the flow of five different types of water based nanofluids due to rotating disk. He employed a spectral Chebyshev collocation method to present numerical solutions of the developed nonlinear problem. The study of nanofluid convective heat transfer has been a popular research topic for the last several years [12–21]. An electrically conducting nanofluid subject to magnetic field, known as ferrofluid, has been found pretty useful in several applications. Ferrofluid comprises of iron based nanoparticles such as magnetite, hematite, cobalt ferrite or some other compounds containing iron. Such iron-based nanoparticles can be used for efficient drug delivery by guiding the particles via external magnets [22, 23]. Particularly, magnetic nanoparticles are prominent in hyperthermia, magnetic cell separation, cancer tumor treatment (radiotherapy and chemotherapy) and contrast enhancement in magnetic resonance imaging (MRI). Jue [24] used semi implicit finite element method in order to simulate magnetic gradient and thermal buoyancy induced cavity ferrofluid flow. Influence of magnetic field dependent viscosity on the horizontal layer of ferrofluid was addressed by Nanjundappa et al. [25]. Natural convection flow of Fe_3O_4-water nanofluid through a rectangular enclosure containing an oval-shaped heat source was considered by Moraveji and Hejazian [26]. MHD flow and heat transfer characteristics in a rotating cylinder was examined by Selimefendigil and Oztop [27]. They observed that cylinder rotation strongly influence the heat transfer rate at low Reynolds number. Ellahi [28] presented the analytical solutions for MHD flow of non-Newtonian nanofluid in a pipe. He also considered temperature dependent viscosity in his analysis. Bahirael and Hangi [29] investigated the heat transfer performance of Mn-Zn ferrite-water ferrofluid in a counter-flow double-pipe heat exchanger under the effect of magnetic field. In another paper, Bahirael et al. [30] examined the flow of Mn-Zn ferrite-water ferrofluid through an annulus under the influence of non-uniform magnetic field. Recently, effect of magnetic field on nanofluid flow and heat transfer has been investigated by several authors [31–40].

To our knowledge, the rotating flow of ferrofluids developed by stretching surface has never been explored. Thus present work is undertaken to fill such a void. Interesting aspect of nonlinear radiative heat transfer is also accounted. This allows us to analyze the problem for both large and small temperature differences between the stretching surface and ambient fluid. Some studies pertaining to the non-linear radiative heat transfer have appeared in the recent past (see [41–46] for details). The governing non-linear differential system has been dealt with

shooting technique combined with Newton method. Emphasis has been given to the role of embedding parameters on the velocity and temperature functions. In shooting method, the boundary conditions are assumed as multivariate functions of the initial conditions at a particular point. It acquires advantage of faster convergence and simple implementation of the methods for initial value problems such as fourth-fifth-order Runge-Kutta (RK45) method.

Mathematical Model

Consider the rotating flow of Fe_3O_4-water ferrofluid caused by a radiative surface coincident with the xy– plane. The surface is subjected to uniform stretch in the x– direction with rate a. The sheet is maintained at a constant temperature T_w whereas T_∞ denotes the temperature outside the thermal boundary layer (see Fig 1). Following the famous Tiwari and Das model [47], the equations embodying the conservation of mass, momentum and energy are expressed as below:

$$\frac{\partial u}{\partial x}+\frac{\partial v}{\partial y}+\frac{\partial w}{\partial z}=0, \tag{1}$$

$$\rho_{nf}\left(u\frac{\partial u}{\partial x}+v\frac{\partial u}{\partial y}+w\frac{\partial u}{\partial z}-2\Omega v\right)=\mu_{nf}\left(\frac{\partial^2 u}{\partial z^2}\right)-\sigma_{nf}{B_0}^2 u, \tag{2}$$

$$\rho_{nf}\left(u\frac{\partial v}{\partial x}+v\frac{\partial v}{\partial y}+w\frac{\partial v}{\partial z}+2\Omega u\right)=\mu_{nf}\left(\frac{\partial^2 v}{\partial z^2}\right)-\sigma_{nf}{B_0}^2 v, \tag{3}$$

$$u\frac{\partial T}{\partial x}+v\frac{\partial T}{\partial y}+w\frac{\partial T}{\partial z}=\alpha_{nf}\left(\frac{\partial^2 T}{\partial z^2}\right)-\frac{1}{(\rho c_p)_{nf}}\frac{\partial q_r}{\partial z}, \tag{4}$$

with the following boundary conditions

$$\begin{aligned} u=u_w=ax, \quad v=0, \quad w=0, \quad T=T_w \quad \text{at} \quad z=0,\\ u=0, \quad v=0, \quad T=T_\infty \quad \text{as} \quad z\to\infty, \end{aligned} \tag{5}$$

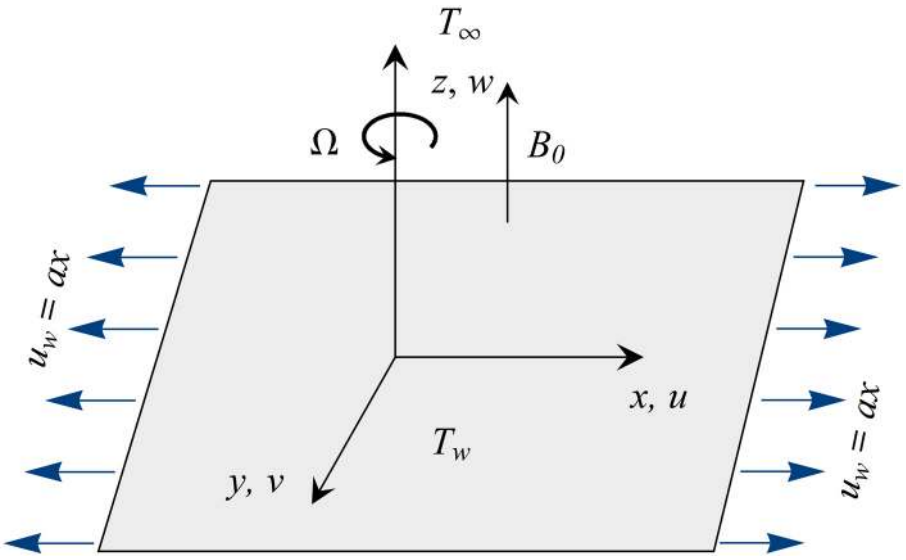

Fig 1. Geometry of the problem and coordinate system.

doi:10.1371/journal.pone.0149304.g001

Table 1. List of symbols.

(x,y,z)	Cartesian coordinate system		*Subscripts*
u,v,w	velocity components along the x-,y-,z- directions respectively	f	fluid phase
T	fluid temperature	s	solid phase
T_w	wall temperature	nf	nanofluid
T_∞	ambient fluid temperature		
u_w	velocity of the stretching sheet		*Greek symbols*
f',g	dimensionless x- and y- components of velocity	λ	ratio of rotation rate to the stretching rate
a	stretching rate	ρ	density
B_0	uniform magnetic field	μ	dynamic viscosity
k	thermal conductivity	v	kinematic viscosity
q_r	radiative heat flux	α	thermal diffusivity
M	Hartman number	Ω	angular velocity
Pr	Prandtl number	σ	electrical conductivity
Rd	radiation parameter	η	similarity variable
Re	Reynolds number	θ	dimensionless temperature
q_w	wall heat flux	θ_w	temperature ratio parameter
Nu	local Nusselt number	ϕ	dimensionless nanoparticle concentration
C_f	skin friction coefficient	τ_{wx},τ_{wy}	wall shear stresses along x– and y– direction

doi:10.1371/journal.pone.0149304.t001

in which u and v are the velocity components along the x– and y– directions respectively, $q_r = -(4\sigma^*/3k^*)\partial T^4/\partial z$ is the Rosseland radiative heat flux in which σ^* is the Stefan-Boltzman constant and k^* is the mean absorption coefficient (see Table 1).

Brinkman [48] expressed the dynamic viscosity of nanofluid μ_{nf} as

$$\mu_{nf} = \frac{\mu_f}{(1-\varphi)^{2.5}}, \tag{6}$$

the effective density ρ_{nf} and effective heat capacity $(\rho c_p)_{nf}$ are expressed as [47]:

$$\rho_{nf} = (1-\phi)\rho_f + \phi\rho_s, \tag{7}$$

$$(\rho c_p)_{nf} = (1-\phi)(\rho c_p)_f + \phi(\rho c_p)_s, \tag{8}$$

We take into account the Maxwell-Garnett model [49] for effective thermal conductivity of nanofluid k_{nf} given below:

$$\frac{k_{nf}}{k_f} = \frac{(k_s+2k_f) - 2\varphi(k_f-k_s)}{(k_s+2k_f) + \varphi(k_f-k_s)}. \tag{9}$$

Moreover, the electrical conductivity of nanofluid σ_{nf} is given in the book by Maxwell [50] as

$$\frac{\sigma_{nf}}{\sigma_f} = 1 + \frac{3(\sigma_s-\sigma_f)\phi}{(\sigma_s+2\sigma_f) - (\sigma_s-\sigma_f)\phi}. \tag{10}$$

In Eqs (6)–(10), ϕ denotes the nanoparticle volume fraction and the subscripts s and f correspond to the solid and fluid phases respectively. Thermophysical properties of water and magnetite-Fe_3O_4 are given in Table 2.

Table 2. Thermo-physical properties of water and magnetite-Fe_3O_4 [10].

	ρ(kg/m^3)	C_p(J/kgK)	K(W/mK)	σ(Ω.m)$^{-1}$
Water	997.1	4179	0.613	0.05
Fe_3O_4	5180	670	9.7	25000

doi:10.1371/journal.pone.0149304.t002

We look for similarity solution of Eqs (1)–(4) in the following forms [5]

$$\eta = \sqrt{\left(\frac{a}{\nu_f}\right)}\, z, \quad u = axf'(\eta), \quad v = axg(\eta), \quad w = -\sqrt{a\nu_f}f(\eta), \qquad T = T_\infty + (T_w - T_\infty)\theta(\eta). \tag{11}$$

In view of the above quantities, the continuity Eq (1) is identically satisfied while Eqs (1)–(5) become

$$\frac{1}{(1-\phi)^{2.5}(1-\phi+\phi\rho_s/\rho_f)}f''' - f'^2 + ff'' + 2\lambda g - \frac{\sigma_{nf}/\sigma_f}{(1-\varphi+\varphi\rho_s/\rho_f)}Mf' = 0, \tag{12}$$

$$\frac{1}{(1-\phi)^{2.5}(1-\phi+\phi\rho_s/\rho_f)}g'' + fg' - f'g - 2\lambda f' - \frac{\sigma_{nf}/\sigma_f}{(1-\varphi+\varphi\rho_s/\rho_f)}Mg = 0, \tag{13}$$

$$\frac{1}{(1-\phi+\phi(\rho c_p)_s/(\rho c_p)_f)}\frac{1}{\mathrm{Pr}}((k_{nf}/k_f + Rd(1+(\theta_w-1)\theta)^3)\theta')' + f\theta' = 0, \tag{14}$$

$$f(0) = 0, \quad g(0) = 0, \quad f'(0) = 1, \quad \theta(0) = 1, \qquad f'(\infty) = 0, \quad g(\infty) = 0, \quad \theta(\infty) = 0, \tag{15}$$

in which $\mathrm{Pr} = (\mu c_p)_f/k_f$ is the Prandtl number of the base fluid, $Rd = 16\sigma^* T_\infty{}^3/3k^* k_f$ denotes the radiation parameter, $M = \sigma B_0^2/\rho_f\Omega$ is the magnetic field parameter and $\lambda = \Omega/a$ is the ratio of rotation rate to the stretching rate. The quantities of practical interest are the skin friction coefficients C_{fx}, C_{fy} and the local Nusselt number Nu_x defined as follows.

$$C_{fx} = \frac{\tau_{wx}}{\rho_f u_w^2}, \quad C_{fy} = \frac{\tau_{wy}}{\rho_f u_w^2}, \quad Nu_x = \frac{xq_w}{k_f(T_w - T_\infty)}, \tag{16}$$

where $\tau_{wx} = \tau_{zx}|_{z=0}$ and $\tau_{wy} = \tau_{zy}|_{z=0}$ are the wall shear stresses and q_w is the wall heat flux given by

$$\tau_{wx} = \mu_{nf}\left.\frac{\partial u}{\partial z}\right|_{z=0}, \quad \tau_{wy} = \mu_{nf}\left.\frac{\partial v}{\partial z}\right|_{z=0}, \quad q_w = -k_{nf}\left.\frac{\partial T}{\partial z}\right|_{z=0} + \left.q_r\right|_{z=0}. \tag{17}$$

Using Eq (11) in Eq (16) one obtains

$$\sqrt{Re_x}C_{fx} = \frac{1}{(1-\phi)^{2.5}}f''(0), \quad \sqrt{Re_x}C_{fy} = \frac{1}{(1-\phi)^{2.5}}g'(0), \quad \frac{Nu_x}{\sqrt{Re_x}} = -\left(\frac{k_{nf}}{k_f} + Rd\theta_w^3\right)\theta'(0), \tag{18}$$

in which $Re_x = u_w x/\nu_f$ is the local Reynolds number.

In the present article, we employed the Tiwari and Das model [47] to address the rotating flow and heat transfer of Fe_3O_4-water ferrofluid driven by a linearly stretching surface.

Table 3. Comparison of current result with previous studies for special cases ($\phi = 0, M = 0$).

λ	Wang [1]		Nazar et al. [3]		Present	
	$f''(0)$	$g'(0)$	$f''(0)$	$g'(0)$	$f''(0)$	$g'(0)$
0	-1	0	-1	0	-1	0
0.5	-1.1384	-0.5128	-1.1384	-0.5128	-1.13838	-0.51276
1.0	-1.3250	-0.8371	-1.3250	-0.8371	-1.32503	-0.837089
2.0	-1.6523	-1.2873	-1.6523	-1.2873	-1.65235	-1.28726

doi:10.1371/journal.pone.0149304.t003

Numerical solutions of the Eqs (12)–(14) subject to the conditions Eq (15) are computed by using shooting method with Runge-Kutta fifth order integration scheme. In all the calculations the volume fraction is considered in the range $0 \leq \phi \leq 0.2$ (as ϕ beyond 0.2 is not physically realizable due to accumulation) while the Prandtl number Pr = 6.2 for water is used. We have compared our results with available studies of Wang [1] and Nazar et al. [3] in the case of pure fluid and found very good agreement (see Table 3).

Numerical Results and Discussion

The numerical values of local Nusselt number $Nu_x/\sqrt{\mathrm{Re}_x}$ for some values of parameters are computed in Table 4. The magnitude of $Nu_x/\sqrt{\mathrm{Re}_x}$ grows sharply with the volume fraction ϕ is when larger wall to ambient temperature ratio is accounted. Moreover $Nu_x/\sqrt{\mathrm{Re}_x}$ has direct as well as non-linearly relationship with the radiation parameter Rd. This outcome is true for both linear and non-linear radiation cases.

Figs 2 and 3 preserve the effects of magnetic field strength on the dimensionless x– and y–components of velocity respectively. The function $g(\eta)$ has a parabolic profile and its value is negative revealing that flow occurs in the negative y– direction. As the Hartman number M enlarges, the flow decelerates in both x– and y– directions. Physically, the presence of magnetic field restricts the fluid motion due to which a thinner boundary layer appears for stronger magnetic field strength.

Table 4. Values of local Nusselt number $Nu_x/\sqrt{Re_x}$ for different values of embedded parameters.

ϕ	M	λ	$Rd = 0$	$Rd = 1$		
				Linear radiation	Nonlinear radiation	
					$\theta_w = 1.1$	$\theta_w = 1.5$
0.1	1	0	1.88862	2.29587	2.36871	2.70039
		0.5	1.85750	2.23679	2.30471	2.60866
		1	1.78831	2.10820	2.16559	2.41046
		2	1.62561	1.82975	1.86624	2.00376
0.1	0	1	1.83496	2.16281	2.22182	2.46987
	0.5		1.81436	2.14190	2.20074	2.45110
	1		1.78831	2.10820	2.16559	2.41046
	2		1.72931	2.02393	2.07670	2.30010
0	1	0.5	1.66171	2.15308	2.23565	2.59822
0.05			1.75604	2.18830	2.26323	2.59451
0.1			1.85750	2.23679	2.30471	2.60866
0.2			2.09314	2.38075	2.43596	2.68996

doi:10.1371/journal.pone.0149304.t004

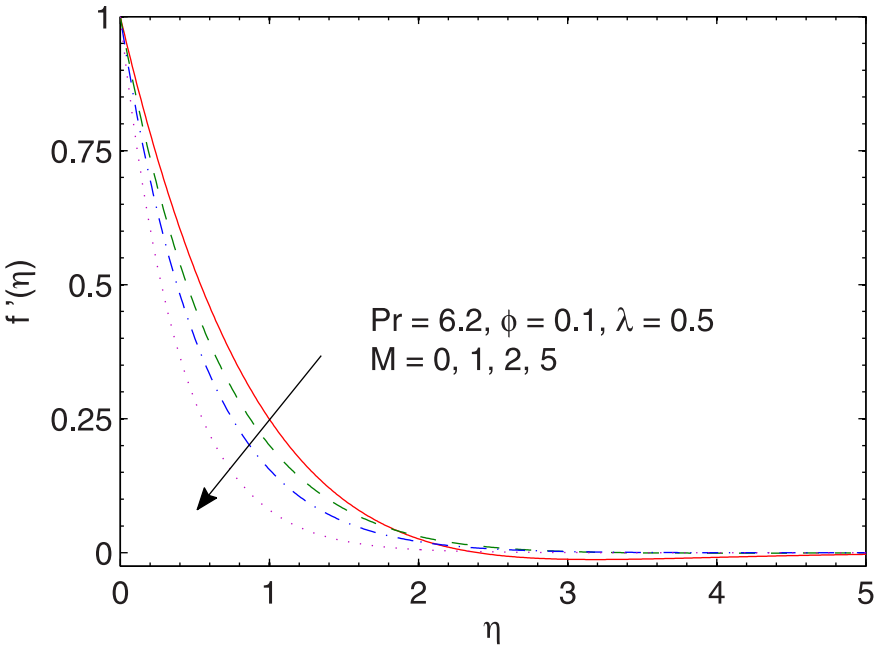

Fig 2. Effect of *M* on $f'(\eta)$.

doi:10.1371/journal.pone.0149304.g002

In Figs 4 and 5, we portray the effects of ratio λ on the x– and y– components of velocity respectively. Larger values of λ indicates smaller stretching rates (along the x– direction) compared to the rotation rate. Due to this fact, the x– component of velocity $f'(\eta)$ is inversely proportional to λ and magnitude of the y– component of velocity $g(\eta)$ increases when λ is increased.

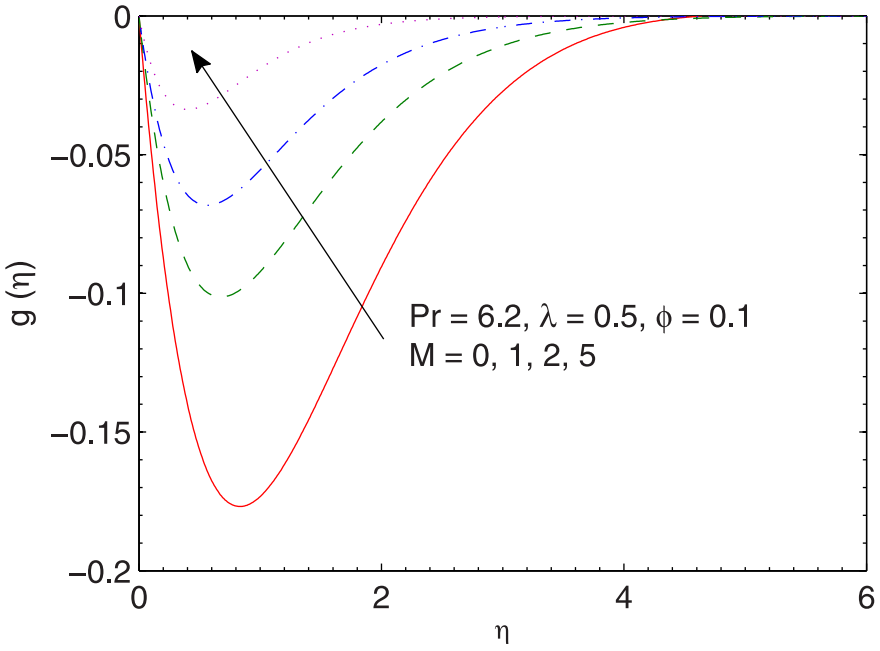

Fig 3. Effect of *M* on $g(\eta)$.

doi:10.1371/journal.pone.0149304.g003

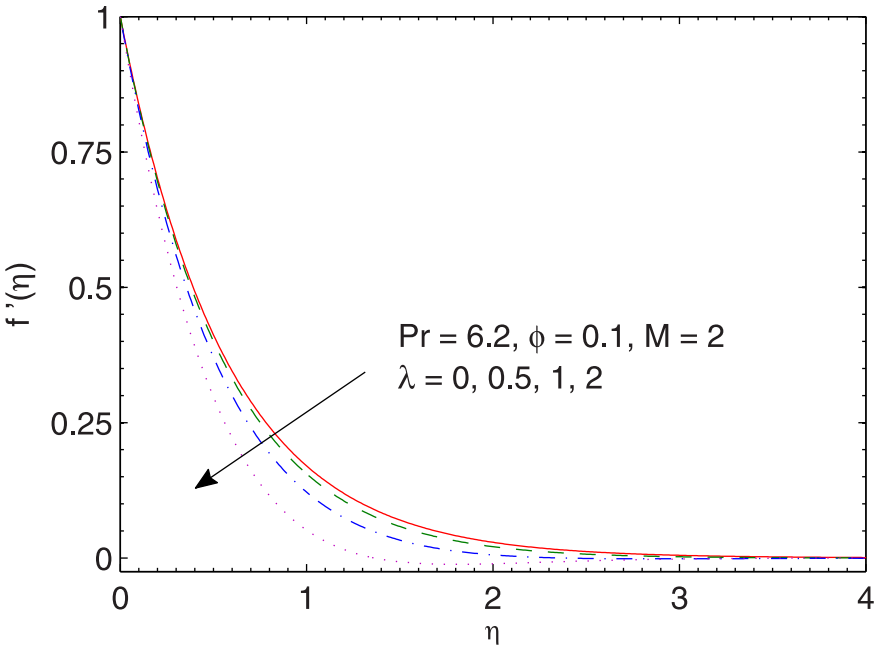

Fig 4. Effect of λ on $f'(\eta)$.

doi:10.1371/journal.pone.0149304.g004

In Figs 6 and 7 we plot the skin friction coefficients $Re_x^{1/2}\ C_{fx}$ and $Re_y^{1/2}\ C_{fy}$ against the volume fraction ϕ for different values of λ. The values of skin friction coefficients $Re_x^{1/2}\ C_{fx}$ and $Re_y^{1/2}\ C_{fy}$ are negative since the fluid applies stress on the stretching wall (that causes the flow). Clearly the magnitudes of $Re_x^{1/2}\ C_{fx}$ and $Re_y^{1/2}\ C_{fy}$ are decreasing functions of M. This is attributed to the fact that transverse magnetic field has a tendency to create a drag (known as

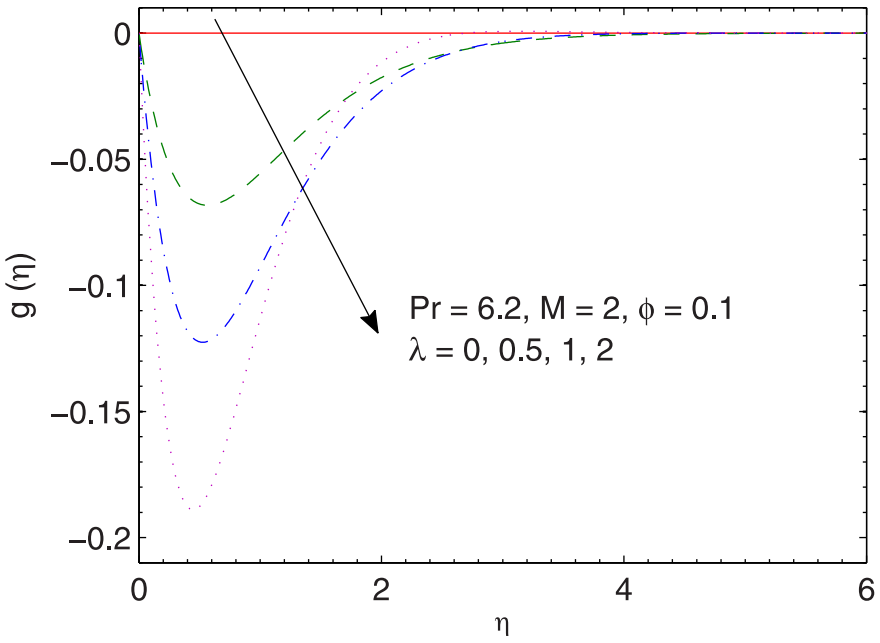

Fig 5. Effect of λ on $g(\eta)$.

doi:10.1371/journal.pone.0149304.g005

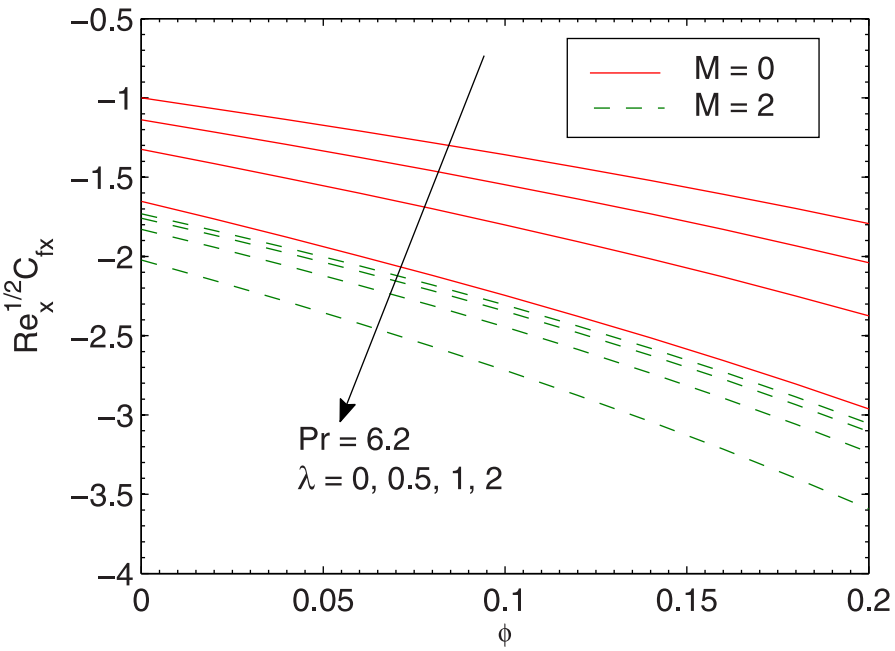

Fig 6. Effect of λ, M and ϕ on $\sqrt{Re_x}C_{fx}$.

doi:10.1371/journal.pone.0149304.g006

Lorentz force that resists the transport phenomenon). This leads to the deceleration of flow and enhancement in the surface shear stress. We also observe that wall shear stresses increase nonlinearly with an increase in ϕ. This means that larger force will be required to displace the fluid over the sheet when larger concentration of Fe_3O_4 particles in water is considered. Physically, an increase in ϕ enhances the viscous force which induces larger stress at the wall (since

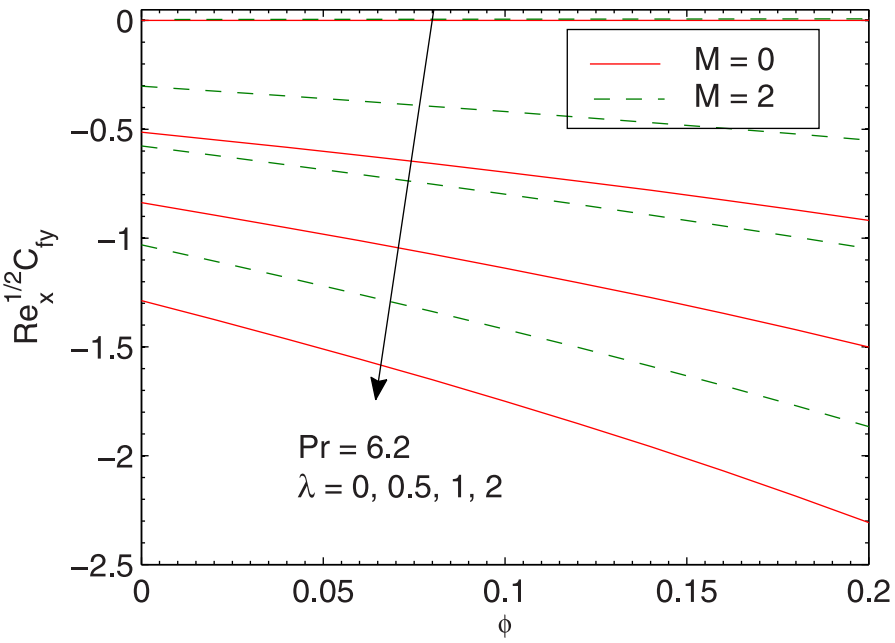

Fig 7. Effect of λ, M and ϕ on $\sqrt{Re_x}C_{fy}$.

doi:10.1371/journal.pone.0149304.g007

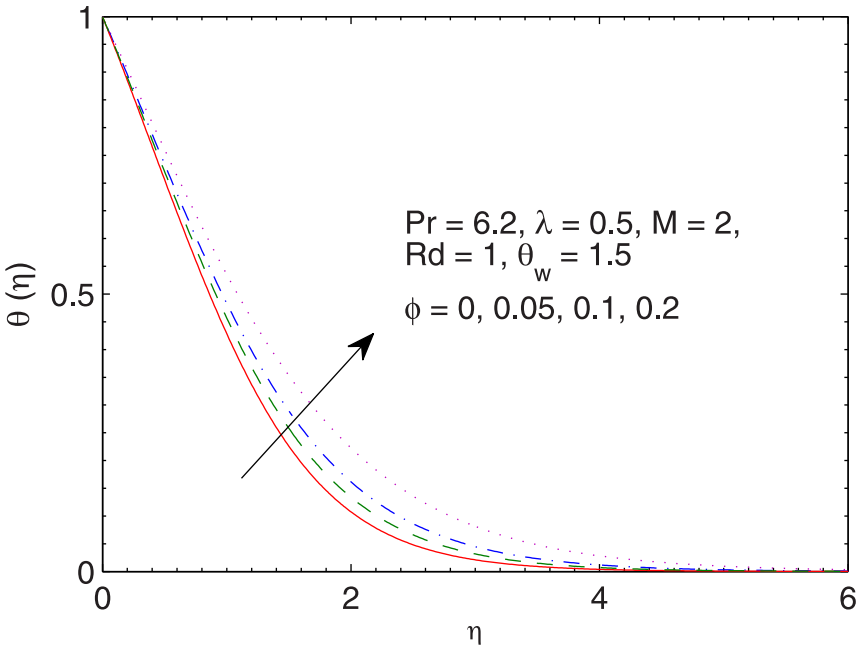

Fig 8. Effect of ϕ on $\theta(\eta)$.

doi:10.1371/journal.pone.0149304.g008

$\tau_{yx} = \mu_{nf}\partial u/\partial y$) and consequently the skin friction coefficient enlarges. The outcome is similar for both magnetic and non-magnetic nanoparticles. We also conclude that tangential stress τ_{zx} is more sensitive to parameter λ than the tangential stress τ_{zy}.

The influence of volume fraction ϕ on the temperature θ is sketched in the Fig 8. As expected, the intense viscous force due to the consideration of large ϕ develops thicker thermal boundary. It is also noted that wall temperature gradient augments with an increase in ϕ.

Fig 9 contains the impact of magnetic field on the temperature θ. The resistance associated with the Lorentz force due to the applied magnetic field enhances the temperature. Due to this reason, temperature rises and thermal boundary layer gets thicker when M is incremented. The behavior of ratio λ on thermal boundary layer is qualitatively similar to that of M (see Fig 10). However the effects are prominently felt when λ is varied.

Temperature profiles for several values of temperature ratio parameter θ_w are sketched in Fig 11. Unlike the linear radiation case, the profiles change from normal shape to the S-shaped thicker profiles when θ_w is increased. Here the thermal boundary layer thickness is controlled by the effective thermal diffusivity $\alpha_{eff} = \alpha + 16\sigma^* T^3/3\rho C_p k^*$) which is a function of temperature. Since the sheet is hotter than the fluid therefore one expects a_{eff} to be larger near the sheet than at the ambient fluid. Due to this reason, an increase in wall to ambient temperature ratio parameter θ_w tends to a decrease the temperature gradient near the surface which results in the point of inflection. More precisely, the concavity of the temperature function changes in $[0,\infty)$ when θ_w is sufficiently large. On the other hand, the concavity has been preserved in case of linear radiation heat transfer. As θ_w enlarges, this corresponds to larger temperature difference between wall and the ambient which eventually imparts a thicker thermal boundary layer. The results are in accordance with the previously published articles.

Fig 12 gives the effect of radiation parameter Rd in both the cases of linear and non-linear radiative heat fluxes. In accordance with Cortell [46], wall slope of temperature tends to a constant finite value when radiation parameter Rd is increased for linear radiation case. Such effect is not preserved in the case of the nonlinear radiation. Temperature θ appears to be larger when

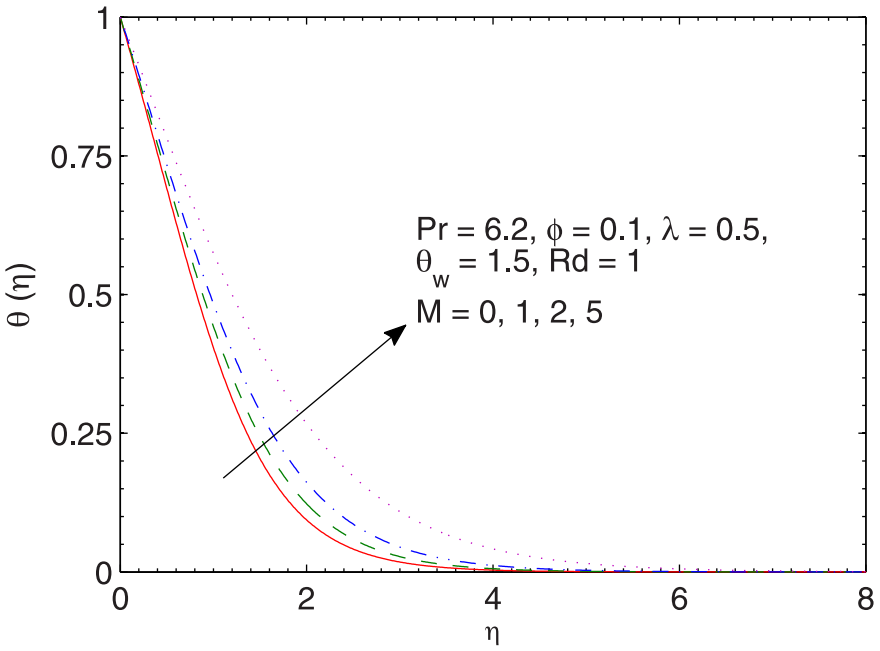

Fig 9. Effect of *M* on *θ*(*η*).

doi:10.1371/journal.pone.0149304.g009

larger radiation parameter is accounted. Moreover, temperature θ rises sharply in non-linear radiation when compared with the linear radiation. From Fig 12 we also envisage that linear and non-linear radiation results are identical only when Rd is small and θ_w is close to one. The difference between linear and non-linear radiation continues to grow as the radiation parameter is gradually increased, a fact that is also found in [45]. Fig 13 shows that local Nusselt number

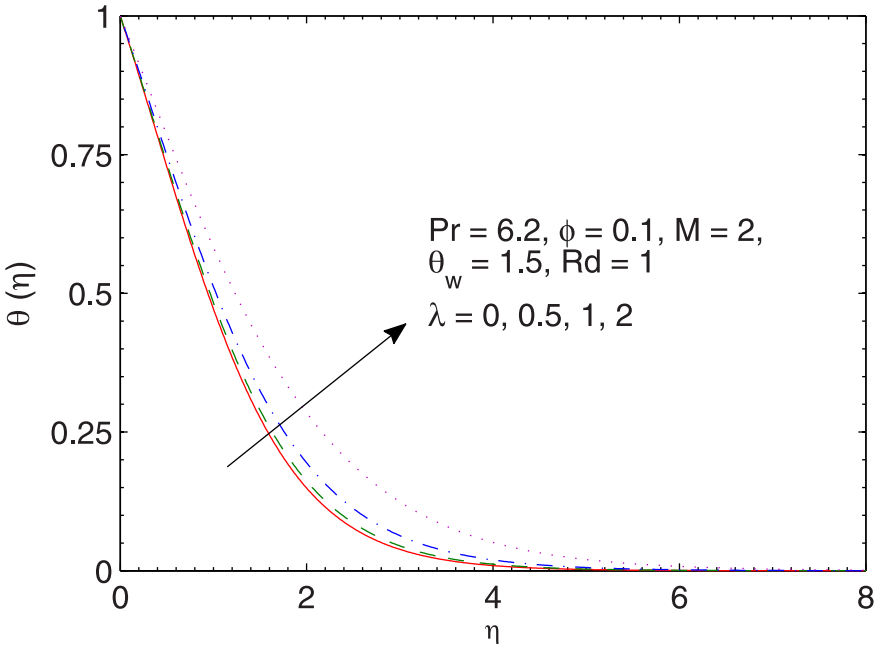

Fig 10. Effect of *λ* on *θ*(*η*).

doi:10.1371/journal.pone.0149304.g010

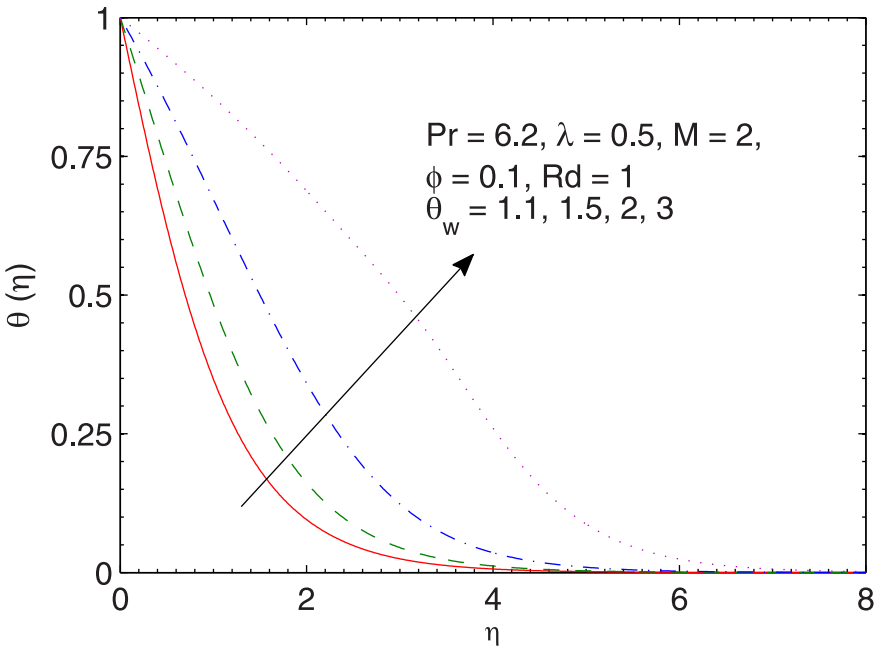

Fig 11. Effect of θ_w on $\theta(\eta)$.

doi:10.1371/journal.pone.0149304.g011

$Nu_x/\sqrt{\mathrm{Re}_x}$ has direct relationship with the volume fraction ϕ is increased. Notably, the heat transfer rate from the sheet significantly varies only for small values of λ. Fig 14 plots the local Nusselt number $Nu_x/\sqrt{\mathrm{Re}_x}$ against θ_w for various values of Rd. We observe a sharp growth in heat transfer rate when θ_w is increased. The slope of this function further increases when Rd is increased. Here the comparison of results for pure water and ferrofluid is also given.

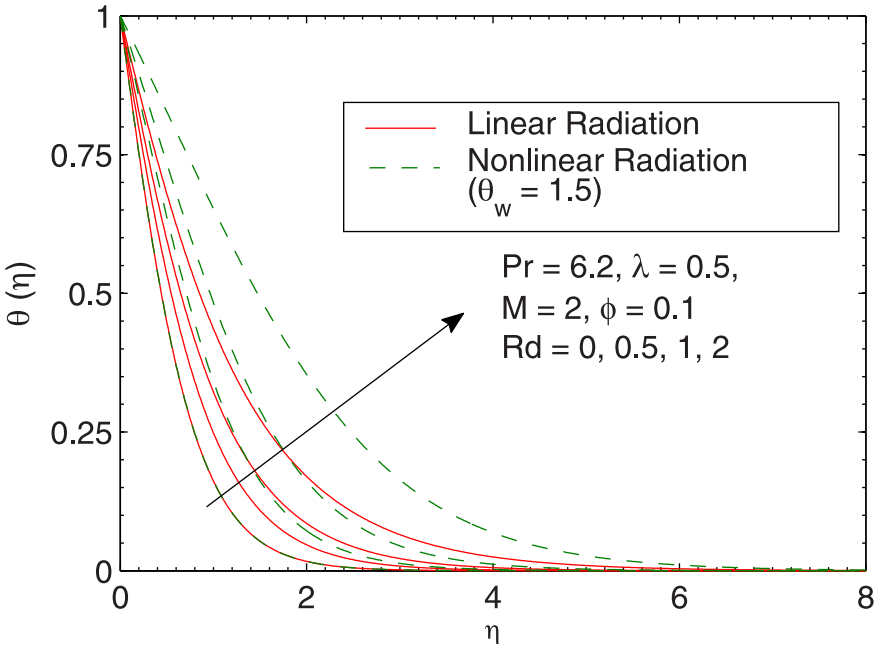

Fig 12. Effect of Rd on $\theta(\eta)$.

doi:10.1371/journal.pone.0149304.g012

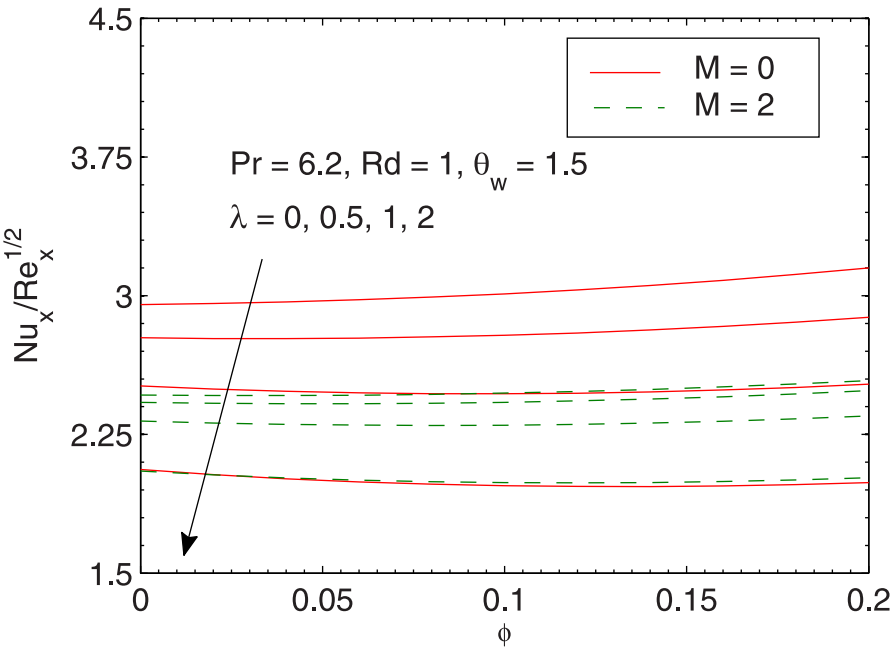

Fig 13. Effects of λ, M and ϕ on $Nu_x/\sqrt{Re_x}$.

doi:10.1371/journal.pone.0149304.g013

Concluding Remarks

Revolving flow and heat transfer of magnetite-water ferrofluid over a deformable surface is explored through Tiwari and Das model. The developed non-linear boundary value problem is tackled by a numerical approach. The major aspects of this work are highlighted below:

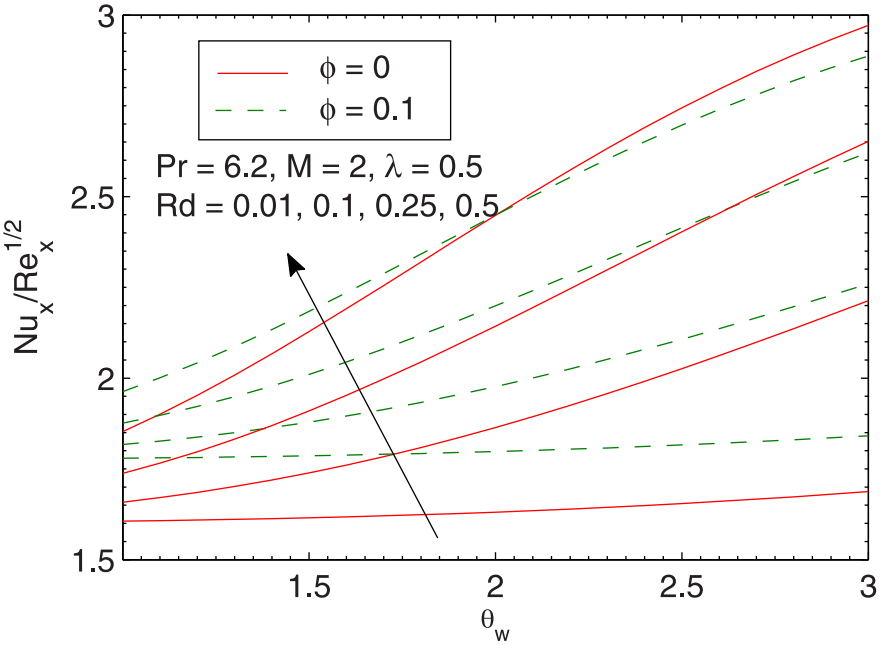

Fig 14. Effects of Rd and θ_w on $Nu_x/\sqrt{Re_x}$.

doi:10.1371/journal.pone.0149304.g014

1. The $y-$ component of velocity is negative and has a parabolic distribution.
2. The parameter λ, which gives the ratio of rotation rate to the stretching rate, has opposite effects on the $x-$ and $y-$ components of velocity qualitatively.
3. For sufficiently large wall to ambient temperature ratio, temperature function θ has an interesting S-shaped profile which indicates the existence of adiabatic case.
4. Variations in $x-$ and $y-$ components of velocity with the nanoparticle volume fraction ϕ is non-monotonic.
5. The velocity distributions f' and g decrease when larger values of magnetic field parameter M are employed.
6. Skin friction coefficient and local Nusselt number are directly proportional to the nanoparticle volume fraction ϕ.
7. Local Nusselt number attenuates when magnetic field strength is intensified.

Acknowledgments

We are thankful to the anonymous referees for their useful comments and suggestions.

Author Contributions

Analyzed the data: AM MM TH. Contributed reagents/materials/analysis tools: AM MM TH AA. Wrote the paper: AM MM TH.

References

1. Wang CY (1988) Stretching a surface in a rotating fluid. ZAMP 39: 177–185.
2. Rajeswari V, Nath G (1992) Unsteady flow over a stretching surface in a rotating fluid. Int. J. Eng. Sci. 30: 747–756.
3. Nazar R, Amin N, Pop I (2004) Unsteady boundary layer flow due to a stretching surface in a rotating fluid. Mech. Res. Commun. 31: 121–128.
4. Hayat T, Javed T, Sajid M (2008) Analytic solution for MHD rotating flow of a second grade fluid over a shrinking surface. Phys. Lett. A 372: 3264–3273.
5. Zaimi K, Ishak A, Pop I (2013) Stretching surface in rotating viscoelastic fluid. Appl. Math. Mech. 34: 945–952.
6. Rashidi MM, Abelman S, Mehr NF (2013) Entropy generation in steady MHD flow due to a rotating porous disk in a nanofluids. Int J. Heat Mass Transf, 62: 515–525.
7. Sheikholeslami M, Hatami M, Ganji DD (2014) Nanofluid flow and heat transfer in a rotating system in the presence of a magnetic field. J. Mol. Liq. 190: 112–120.
8. Mustafa M (2015) Cattaneo-Christov heat flux model for rotating flow and heat transfer of upper-convected Maxwell fluid. AIP Advances 5: doi: 10.1063/1.4917306
9. Choi SUS, Eastman JA (1995) Enhancing thermal conductivity of fluids with nanoparticles. in: The Proceedings of the 1995 ASME International Mechanical Engineering Congress and Exposition, San Francisco, USA, ASME, FED 231/MD 66: 99–105.
10. Sheikholeslami M, Ganji DD (2014) Ferrohydrodynamic and magnetohydrodynamic effects on ferrofluid flow and convective heat transfer. Energy 75: 400–410.
11. Turkyilmazoglu M (2014) Nanofluid flow and heat transfer due to a rotating disk. Comp. Fluids 94: 139–146.
12. Kuznetsov AV, Nield DA (2014) Natural convective boundary-layer flow of a nanofluid past a vertical plate: A revised model. Int J Therm Sci 77: 126–129.
13. Rashidi MM, Abelman S, Mehr NF (2013) Entropy generation in steady MHD flow due to a rotating porous disk in a nanofluid. Int. J. Heat Mass Transf. 62: 515–525.

14. Sheikholeslami M, Sheykholeslami FB, Khoshhal S, Mole-Abasia H, Ganji DD, Rokni HB (2014) Effect of magnetic field on Cu—water nanofluid heat transfer using GMDH-type neural network. Neural Comput. Appl. 25: 171–178.
15. Malvandi A, Ganji DD (2014) Magnetic field effect on nanoparticles migration and heat transfer of water/alumina nanofluid in a channel. J. Magnet. Magn. Mater. 362: 172–179.
16. Mushtaq A, Mustafa M, Hayat T, Alsaedi A (2014) Nonlinear radiative heat transfer in the flow of nanofluid due to solar energy: A numerical study. J. Taiwan Inst. Chem. Eng. 45: 1176–1183.
17. Rashidi MM, Freidoonimehr N, Hosseini A, Bég OA, Hung TK (2014) Homotopy simulation of nanofluid dynamics from a non-linearly stretching isothermal permeable sheet with transpiration. Meccan. 49: 469–482.
18. Nield DA, Kuznetsov AV (2014) Forced convection in a parallel-plate channel occupied by a nanofluid or a porous medium saturated by a nanofluid. Int. J. Heat Mass Transf. 70: 430–433.
19. Mustafa M, Khan JA (2015) Model for flow of Casson ferrofluid past a non-linearly stretching sheet considering magnetic field effects. AIP Adv. 5: doi: 10.1063/1.4927449
20. Khan JA, Mustafa M, Hayat T, Sheikholeslami M, Alsaedi A (2015) Three-dimensional flow of nanofluid induced by an exponentially stretching sheet: An application to solar energy. PLoS ONE 10: doi: 10.1371/journal.pone.0116603
21. Mustafa M, Khan JA, Hayat T, Alsaedi (2015) On Bödewadt flow and heat transfer of nanofluids over a stretching stationary disk. J. Mol. Liq. 211: 119–125.
22. Tangthieng C, Finlayson BA, Maulbetsch J, Cader T (1999) Heat transfer enhancement in ferrofluids subjected to steady magnetic fields. J. Magn. Magn. Mater. 201: 252–255.
23. Rosensweig R (2002), Heating magnetic fluid with alternating magnetic field. J. Magn. Magn. Mater. 252 370–374.
24. Jue TC (2006) Analysis of combined thermal and magnetic convection ferrofluid flow in a cavity. Int. Commun. Heat Mass Transf. 33: 846–852.
25. Nanjundappa CE, Shivakumara IS, Ravisha MM (2010) The onset of ferroconvection in a horizontal ferrofluid saturated porous layer heated from below and cooled from above with constant heat flux subject to MFD viscosity. Int. Commun. Heat Mass Transf. 37: 1246–1250.
26. Moraveji MK, Hejazian M (2013) Natural convection in a rectangular enclosure containing an oval-shaped heat source and filled with Fe_3O_4-water nanofluids. Int. Commun. Heat Mass Transf. 44: 135–146.
27. Selimefendigil F, Oztop HF (2014) Effect of a rotating cylinder in forced convection of ferrofluid over a backward facing step. Int. J. Heat Mass Transf. 71: 142–148.
28. Ellahi R (2013) The effects of MHD and temperature dependent viscosity on the flow of non-Newtonian nanofluid in a pipe: Analytical solutions. Appl. Math. Model. 37: 1451–1467.
29. Bahiraei M, Hangi M (2013) Investigating the efficacy of magnetic nanofluid as a coolant in double-pipe heat exchanger in the presence of magnetic field. Energy Conversion and Management 76: 1125–1133.
30. Bahiraei M, Hosseinalipour SM, Hangi M (2014) Numerical study and optimization of hydrothermal characteristics of Mn—Zn ferrite nanofluid within annulus in the presence of magnetic field. J. Supercond Nov. Magn. 27: 527–534.
31. Azizian R, Doroodchi E, McKrell T, Buongiorno J, Hu LW, Moghtaderi B (2014) Effect of magnetic field on laminar convective heat transfer of magnetite nanofluids. Int. J. Heat Mass Transf. 68: 94–109.
32. Sheikholeslami M, GorjiBandpy M, Ellahi R, Zeeshan A (2014) Simulation of MHD CuO—water nanofluid flow and convective heat transfer considering Lorentz forces. J. Magn. Magn. Mater. 369: 69–80.
33. Malvandi A, Ganji DD (2014) Magnetic field effect on nanoparticles migration and heat transfer of water/alumina nanofluid in a channel. J. Magnet. Magn. Mater. 362: 172–179.
34. Zhang X, Huang H (2014) Effect of magnetic obstacle on fluid flow and heat transfer in a rectangular duct. Int.Commun. Heat Mass Transf. 51: 31–38.
35. Bahiraei M, Hangi M (2015) Flow and heat transfer characteristics of magnetic nanofluids: A review. J. Magn. Magn Mater. 374: 125–138.
36. Bahiraei M (2015) Effect of particle migration on flow and heat transfer characteristics of magnetic nanoparticle suspensions. J. Mol. Liq. 209: 531–538.
37. Sheikholeslami M, Rashidi MM, Ganji DD (2015) Numerical investigation of magnetic nanofluid forced convective heat transfer in existence of variable magnetic field using two phase model. J. Mol. Liq. 212: 117–126.
38. Sheikholeslami M, Rashidi MM, Ganji DD (2015) Effect of non-uniform magnetic field on forced convection heat transfer of Fe3O4- water nanofluid. Comput. Methods Appl. Mech. Engg. 294: 299–312.

39. Sheikholeslami M, Ellahi R (2015) Three dimensional mesoscopic simulation of magnetic field effect on natural convection of nanofluid. Int. J. Heat Mass Transf. 89: 799–808.

40. Sheikholeslami M, Vajravelu K, Rashidi MM (2016) Forced convection heat transfer in a semi annulus under the influence of a variable magnetic field. Int. J. Heat Mass Transf. 92: 339–348.

41. Rahman MM, Eltayeb IA (2013) Radiative heat transfer in a hydromagnetic nanofluid past a non-linear stretching surface with convective boundary condition. Meccan. 48: 601–615.

42. Pantokratoras A, Fang T (2014) Blasius flow with non-linear Rosseland thermal radiation. Meccan. 49: 1539–1545.

43. Mushtaq A, Mustafa M, Hayat T, Alsaedi A (2014) Effects of thermal radiation on the stagnation-point flow of upper-convected Maxwell fluid over a stretching sheet. J Aerosp Engg 27: doi: 10.1061/(ASCE)AS.1943-5525.0000361

44. Mustafa M, Mushtaq A, Hayat T, Ahmad B (2014) Nonlinear radiation heat transfer effects in the natural convective boundary layer flow of nanofluid past a vertical plate: a numerical study. PLoS ONE 9: doi: 10.1371/journal.pone.0103946

45. Mushtaq A, Mustafa M, Hayat T, Alsaedi A (2014) On the numerical solution of the nonlinear radiation heat transfer problem in a three-dimensional flow. Z. Naturforsch. 69: 705–713.

46. Cortell R (2014) MHD (magneto-hydrodynamic) flow and radiative nonlinear heat transfer of a visco-elastic fluid over a stretching sheet with heat generation/absorption. Energy 74: 896–905.

47. Tiwari RK, Das MK (2007) Heat transfer augmentation in a two-sided lid-driven differentially heated square cavity utilizing nanofluids. Int. J. Heat Mass Transf. 50: 2002–2018.

48. Brinkman HC (1952) The viscosity of concentrated suspensions and solutions. J. Chem. Phys. 20: 571–581.

49. Khanafer K, Vafai K, Lightstone M (2003) Buoyancy-driven heat transfer enhancement in a two-dimensional enclosure utilizing nanofluids. Int. J. Heat Mass Transf. 46: 3639–3653.

50. Maxwell JC (1904) A treatise on electricity and magnetism. Cambridge Oxford University Press.